

Retrieval of the ultraviolet aerosol optical depth during a spring campaign in the Bavarian Alps

Jacqueline Lenoble, Timothy Martin, Mario Blumthaler, Rolf Philipona, Astrid Albold, Thierry Cabot, Alain de La Casinière, Julian Gröbner, Dominique Masserot, Martin Müller, Thomas Pichler, Günther Seckmeyer, Daniel Schmucki, Mamadou Lamine Touré, and Alexis Yvon

A measurement campaign was organized in March 1999 in the Bavarian Alps as part of the European project, Characteristics of the UV Radiation Field in the Alps (CUVRA), to analyze the effect of altitude, aerosols, and snow cover on ground-level UV spectral irradiance. We present the results of simultaneous measurements of aerosol optical depth (AOD) made at various sites on two cloudless days in March 1999. The two days exhibited different aerosol conditions. Results derived from spectral measurements of UV irradiance are compared with data from filter radiometer measurements made at discrete wavelengths extending from the UV to the near IR. The different methods generated values for the AOD that were in good agreement. This result confirms that one can use either method to retrieve the AOD with an uncertainty of approximately 0.03–0.05. On 18 March, high turbidity was observed at low altitude (400-nm AOD \sim 0.5 at 700 m above sea level), and the AOD decreased regularly with altitude; on 24 March, the turbidity was much less (0.11 at 700 m above sea level). On both days very low AODs (0.05–0.09) were measured at 3000 m above sea level. The spectral dependence of the AOD is often parameterized by the angstrom relationship; the α parameter is generally difficult or impossible to retrieve from spectral measurements because of the relatively narrow wavelength range (320–400 nm), and only one of the spectroradiometers used during the campaign permits this retrieval. In most cases, during this field campaign, α was found by filter sunphotometers to be 1.1–1.5. © 2002 Optical Society of America
OCIS codes: 010.1100, 010.1310, 120.5630, 300.6540.

1. Introduction

UV radiation, particularly the shorter UV-B wavelengths, that reaches the Earth's surface can be

J. Lenoble (jacqueline.lenoble@ujf-grenoble.fr) and D. Masserot are with the Laboratoire d'Optique Atmosphérique, Université des Sciences et Technologies de Lille, Lille, France; J. Lenoble is also with the Equipe Interactions Rayonnement Solaire Atmosphère, Université Joseph Fourier, Grenoble, France. At the time of this research, T. Martin, A. Albold, and M. Müller were with the Fraunhofer Institute für Umweltforschung, Garmisch-Partenkirchen, Germany; T. Martin is now with the Institute of Geophysics, Astrophysics and Meteorology, University of Graz, Graz, Austria. At the time of this research, M. Blumthaler, J. Gröbner, and T. Pichler were with the Institute of Medical Physics, Innsbruck, Austria; J. Gröbner is now with the Joint Research Center, Environment Institute, Ispra, Italy. R. Philipona and D. Schmucki are with the Physikalisch-Meteorologisches Observatorium, Davos, Switzerland. T. Cabot, A. de La Casinière, M. L. Touré, and A. Yvon are with the Equipe Interactions Rayonnement Solaire Atmosphère, Université Joseph Fourier, Grenoble, France. G. Seckmeyer is with the Institute for Meteorology and Climatology, University of Hannover, Hannover, Germany.

Received 30 July 2001; revised manuscript received 18 October 2001.

0003-6935/02/091629-11\$15.00/0

© 2002 Optical Society of America

harmful to vegetation, including agriculture and forestry, and to wild and domestic animals.¹ The effects of UV radiation can be particularly severe in mountainous regions because of the thinner atmosphere and cleaner air that are found there and, in winter, because of multiple reflection of radiation between the snow-covered ground and the atmosphere. In the course of many outdoor activities pursued in mountainous terrains, human beings may be exposed to significant UV doses in these regions. A precise knowledge of UV irradiance and of its dependence on factors such as ozone, clouds, altitude, aerosols, and surface reflectance is desirable, therefore. An investigation of the UV radiation environment in the Bavarian Alps was conducted within the European project Characterization of the UV Radiation Field in the Alps (CUVRA).

As part of the CUVRA project, a coordinated measurement campaign took place within the region of Garmisch-Partenkirchen, Southern Germany, from 13 to 24 March 1999. Several UV spectroradiometers, sunphotometers, and broadband radiometers were operated at different altitudes; a complete description of the campaign and a general review of the results can be found in Ref. 2. The main objectives

Table 1. Organizations and Instruments Involved in AOD Measurements

Organization	Spectroradiometer ^a	Filter Radiometer
IFU ^b	DEG, DEZ	
UI ^c	ATI	Microtops
UJF ^d	FRG	
USTL ^e		Cimel
PMOD/WRC ^f		2 PFRs ^g

^aSpectroradiometer names are not acronyms but just references (DE stands for Deutschland): DEG, instrument used at Garmisch; DEZ, instrument at Zugspitze; ATI, instrument from Austria (Innsbruck); FRG, instrument from France (Grenoble).

^bFraunhofer Institut für Umweltforschung, Germany.

^cInstitute of Medical Physics, University of Innsbruck, Innsbruck, Austria.

^dUniversité Joseph Fourier, Grenoble, France.

^eUniversité des Sciences et Technologies de Lille, France.

^fPhysikalisch-Meteorologisches Observatorium Davos/World Radiation Center, Switzerland.

^gPrecision filter radiometers.

of the campaign were analysis of the variation of UV irradiance with altitude and examination of the influence of snow-covered ground on the received radiation. Atmospheric aerosols are an important modulator of UV irradiance (see, e.g., Ref. 3). During the campaign, various methods were employed to measure the aerosol optical depth (AOD) and to extract information about the physical properties of the aerosols. In this paper we compare the results of the measuring methods and examine the extent to which information about the properties of the atmospheric aerosol can reliably be retrieved; we present the results for two cloudless days. We hope that these data, although they are limited, may make a useful contribution to the knowledge of aerosol climatology that is necessary for climate studies,⁴ such as in remote sensing of the Earth's surface and atmosphere.⁵

We compare two approaches to retrieving the AOD. Filter radiometers (or sunphotometers) that measure direct solar irradiance at a few discrete channels across a wide range of wavelengths are specifically designed for obtaining the AOD; an important question is how their data can be extrapolated to UV wavelengths. A second approach utilizes measurements of the direct component of irradiance by UV spectroradiometers to derive a spectral distribution of the AOD over a limited wavelength range; the results are compared with those of AODs from the sunphotometers.

In Section 2 we present the method and the instruments used during the campaign for measuring the AOD at the different measurement sites; the results are described in Section 3 and summarized in Section 4. In Section 5 we present some modeling of the aerosols; our conclusions are given in Section 6.

2. Presentation of the Method and of the Instruments

The AOD measurements use the extinction of the direct solar irradiance through the atmosphere; the method is summarized in Appendix A. The measurements are restricted to times when clouds do not obscure the Sun.

During the CUVRA campaign, cloudless days occurred only on 18, 24, and 25 March 1999, although direct-Sun observations were possible on other occasions when the cloud cover was not complete.

Filter radiometers or sunphotometers were used specifically to measure the AOD across a wide range of discrete wavelengths. With interpolation or extrapolation of these data, a result at a general UV wavelength could be obtained. These instruments can be divided into two categories: regular commercial sunphotometers (to which we refer in what follows as sunphotometers) and special precision filter radiometers (PFRs); these instruments are described in Subsections 2.A and 2.B, respectively.

In contrast, spectroradiometers are designed to measure spectral UV irradiance. With measurements of direct UV irradiance these instruments can in principle permit the retrieval of the aerosol optical depth across the whole of the measured wavelength range. The spectroradiometers are described in Subsection 2.C.

In Table 1 we list the organizations that participated in the AOD measurement campaign; their instruments and acronyms are defined; Table 2 lists the stations where measurements were performed, with their altitudes, and the instruments used at those stations.

A. Commercial Sunphotometers

The University of Lille operated a sunphotometer built by the Cimel Company. This is a hand-held instrument pointed manually toward the Sun, with 10-nm-wide filters centered at 440, 670, 870, and 1020 nm; it is similar in its design to the sunphotometer part of the automatic Cimel instrument described by Holben *et al.*⁶ It was calibrated by use of Langley plots at the Zugspitze station under clear

Table 2. Measurement Sites and Instruments

Site	Altitude (asl, m)	Spectroradiometer	Filter Radiometer (Dates Used)
Murnau	650		Cimel (13, 24, and 25 March)
Garmisch	730	DEG	PFR
Seefeld	1200	ATI	Cimel (10, 24, and 25 March)
Wank	1730	FRG	Microtops
Zugspitze	2964	DEZ	Cimel (17, 24, and 25 March)
			PFR
			Cimel (18 March)

and stable atmospheric conditions. Measurements were performed on different days (see Table 2) at Murnau, Garmisch-Partenkirchen, Wank, and Zugspitze; several readings were made over periods of 3 or 4 minutes and were averaged. The uncertainty of AODs measured with the Cimel instrument was estimated to be ± 0.03 and was due to inaccuracies in calibration. Another hand-held sunphotometer, made by Microtops, with filters at 340, 380, 440, 500, and 675 nm (with widths of 2, 4, 10, 10, and 10 nm, respectively), operated by the University of Innsbruck (UI), measured all five channels simultaneously. The uncertainty was estimated by scientists at the UI to be ± 0.02 . This instrument recorded the AOD at the UI's station at Seefeld on all clear days. It was later recalibrated during a campaign at Jungfraujoch [3576 m above sea level (asl)] in the summer of 1999; the changes in the zero air-mass intercept were less than $\pm 3\%$.

B. Precision Filter Radiometers

The Physikalisch-Meteorologisches Observatorium Davos/World Radiation Center (PMOD/WRC) used precision filter radiometers to measure direct solar UV as well as visible shortwave radiation; during this campaign, only the visible shortwave PFRs were used for determination of AOD at four fixed wavelengths. The PFR instrument had four independent channels, centered at wavelengths 368, 412, 500, and 862 nm as recommended by the World Meteorological Organization for aerosol measurements. This instrument is equipped with 5-nm-wide dielectric interference filters.

The precision filter radiometers were designed with emphasis on instrumental stability. The detectors are kept in a controlled environment and exposed to solar radiation only during actual measurements. The PFR is housed in a weatherproof tube of 88-mm diameter and 390-mm length with an entrance window of synthetic quartz and a weight of 3 kg. The tube is hermetically sealed and maintains an internal atmosphere of dry nitrogen. The temperature of the detector head is stabilized at 20 ± 0.1 °C by an active Peltier-type thermostatic controller over an ambient temperature range from -20 to $+35$ °C. An internal shutter opens for a few seconds every 2 min to keep dose-related degradation to a minimum. Two apertures define a field of view of 2.5° and a slope angle of 0.7° , and an optical position sensor accurately monitors the solar pointing within a $\pm 0.7^\circ$ range.

A CR10 data acquisition system (Campbell Scientific, Leicestershire, UK) is an integral part of the PFR instrument. It performs simultaneous measurements of the photometric and various housekeeping signals while controlling the shutter and measuring sequence. During the CUVRA campaign the period between measurements was set to 1 min. Precision filter radiometers were designed as reference instruments for accurate AOD determination within the Global Atmosphere Watch program; PMOD/WRC is acting as a world optical depth re-

search and calibration center and maintains a PFR laboratory calibration facility at Davos, Switzerland, and a test facility for Langley calibration on the Jungfraujoch at 3580 m asl. Each instrument is first characterized and calibrated in the laboratory with the PMOD/WRC reference standard lamp. To back up the stability and accuracy of the lamp calibration a trap detector is used with a calibration that is traceable to the Physikalisch-Technische Bundesanstalt at Berlin. Each instrument was tested at Jungfraujoch and calibrated from Langley plots; a reference instrument is located permanently there, and calibrations are made whenever possible. The accuracy of AOD is estimated to be 0.01 or better for all wavelengths.

Two sets of PFRs were used during the campaign, one at the Fraunhofer Institute site at Garmisch-Partenkirchen and the other at Zugspitze. The PFRs were mounted on solar trackers, and data from all channels were recorded simultaneously every minute.

C. UV Spectroradiometers

Of the seven spectroradiometers used during the campaign, four measured the direct solar irradiance. Two instruments operated by the Fraunhofer Institute, one (DEG) at the institute site in Garmisch-Partenkirchen (altitude 730 m asl) and the other (DEZ) at Zugspitze (2964 m asl), measured the direct irradiance. The University of Innsbruck instrument (ATI) measured the irradiance at Seefeld (1200 m asl). These three instruments are Bentham DM-300 spectrometers; the DEG and the DEZ use solar pointing collimators made from long tubes with baffles to limit the field of view to approximately 2° ; the ATI uses a telescope with a field of view of $\sim 1.5^\circ$.

The University of Grenoble instrument (FRG) is a Bentham DM-150 spectrometer that is operated at Wank (1730 m asl). It measures the diffuse irradiance with a shadow disk ($\sim 13^\circ$ field of view), and the direct irradiance is obtained as the difference between the global and the diffuse irradiance.

The four instruments measured the spectral irradiance every 30 min, from 290 to 400 nm, with a resolution (PWHM) of 0.8 nm for the FRG instrument and 0.42 nm for the others. The instruments were calibrated in a darkroom before the campaign by use of the same standard lamp (a 1-kW FEL lamp with a calibration certificate issued by the U.S. National Institute of Standards and Technology). For a further check on the reliability of the measurements, the instruments also made simultaneous measurements of global irradiance at the Garmisch site for the first three days of the campaign.² The DEG, DEZ, ATI, and FRG instruments produced measurements that agreed to within 5% down to 300 nm, which is reasonable for this type of measurement. Adding the different sources of error, Bernhard and Seckmeyer⁷ estimated the uncertainty to be $\sim 6\%$ in the UV-A and 13% at 300 nm for this type of measurement. Similar precision is expected in direct and diffuse irradiance measurements.

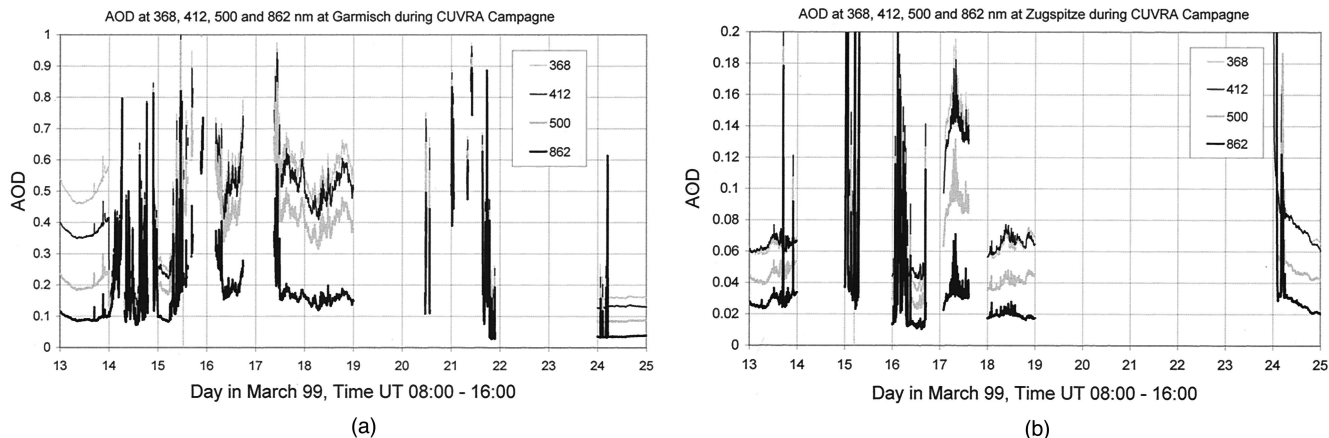


Fig. 1. Time series of AOD measured during the CUVRA campaign by PFRs at four wavelengths at Garmisch and at Zugspitze. The gaps in the curves correspond to periods when the Sun was obscured by cloud.

3. Results

Figure 1 shows the variation of the AOD at Garmisch-Partenkirchen and at Zugspitze measured by PFRs during the entire campaign. The AOD values show large oscillations that were most likely due to thin clouds, but generally they increased during the first part of the campaign (13–18 March); very few measurements from 19 to 22 March are available because the weather was bad, with the sky almost continuously overcast. The results analyzed in this paper concern mostly 18 and 24 March, which were almost completely cloudless at all stations; March 18 was more turbid (larger AOD) than March 24.

A. AODs and Angstrom Parameters from Filter Radiometers

The spectral distributions of the AOD, $\tau(\lambda)$, obtained from measurements at different wavelengths across a large wavelength interval by the Cimel and the Microtops sunphotometers and by the two PFRs were fitted according to the empirical angstrom relationship

$$\tau(\lambda) = \beta\lambda^{-\alpha}, \quad (1)$$

where λ is given in micrometers and α and β are free parameters. This procedure permits the interpolation or extrapolation of the measurement to a common wavelength, which is necessary for comparison.

Here we have chosen to present the AOD at 400 nm because this wavelength, which is the limit of the UV spectral measurements, needs no extrapolation of the PFR or of the Microtops values and only a small extrapolation for the Cimel values. The spectral variation of AOD (roughly captured by the parameter α) contains information on the type of aerosol, which is discussed in Section 5 below.

1. PFR Results (Garmisch and Zugspitze)

The PFR data consisted of values of the AOD at the four channels, recorded every minute; the high frequency of these measurements provides a good basis for defining periods of atmospheric stability. Figure

2 shows the time series of AOD for Garmisch and Zugspitze on 18 and 24 March.

On 18 March the PFR at Garmisch [Fig. 2(a)] showed rapid oscillations of small amplitude superposed upon a larger feature, with a minimum occurring at $\sim 10:00$ UT and a maximum near 14:30, visible at the shortest wavelengths. Above Zugspitze [Fig. 2(b)] the AODs were almost a tenth of the Garmisch values, with small oscillations. The Zugspitze AOD at 368 nm was somewhat smaller than the AOD at 412 nm; this result shows that the angstrom relationship must be treated with caution, as we discuss below.

On 24 March the PFR data showed the passage of some clouds at both stations before 10:00; after that time the AODs were very stable at Garmisch [Fig. 2(c)], with values much smaller than on 18 March. At Zugspitze [Fig. 2(d)] the AOD decreased slowly and steadily through the day; the values were almost the same at 368 and 412 nm. Table 3 lists the average AODs with their standard deviations for the four cases; the standard deviations are most likely due to the natural variability of the AOD, with possibly a small contribution of random uncertainty in the AOD measurements; their small values (less than 10%) are consistent with the expected precision of the AODs. The AOD values, interpolated to 400 nm, and those of the α parameter are also listed in Table 3; the AODs at 400 nm are shown in Fig. 3, in which the results for the instruments from different stations are compared.

2. Cimel Results for the Several Stations

Table 4 summarizes the measurements performed at various sites with the Cimel instrument; several successive readings were averaged, and their standard deviation ($\sim 10\%$) was taken as the uncertainty in the AOD. The four channel values were fitted to the angstrom relationship, and the results given are the α and β values; the values of AOD at 400 nm, obtained by extrapolation, are listed in Table 4 and, for 18 and 24 March, compared in Fig. 3.

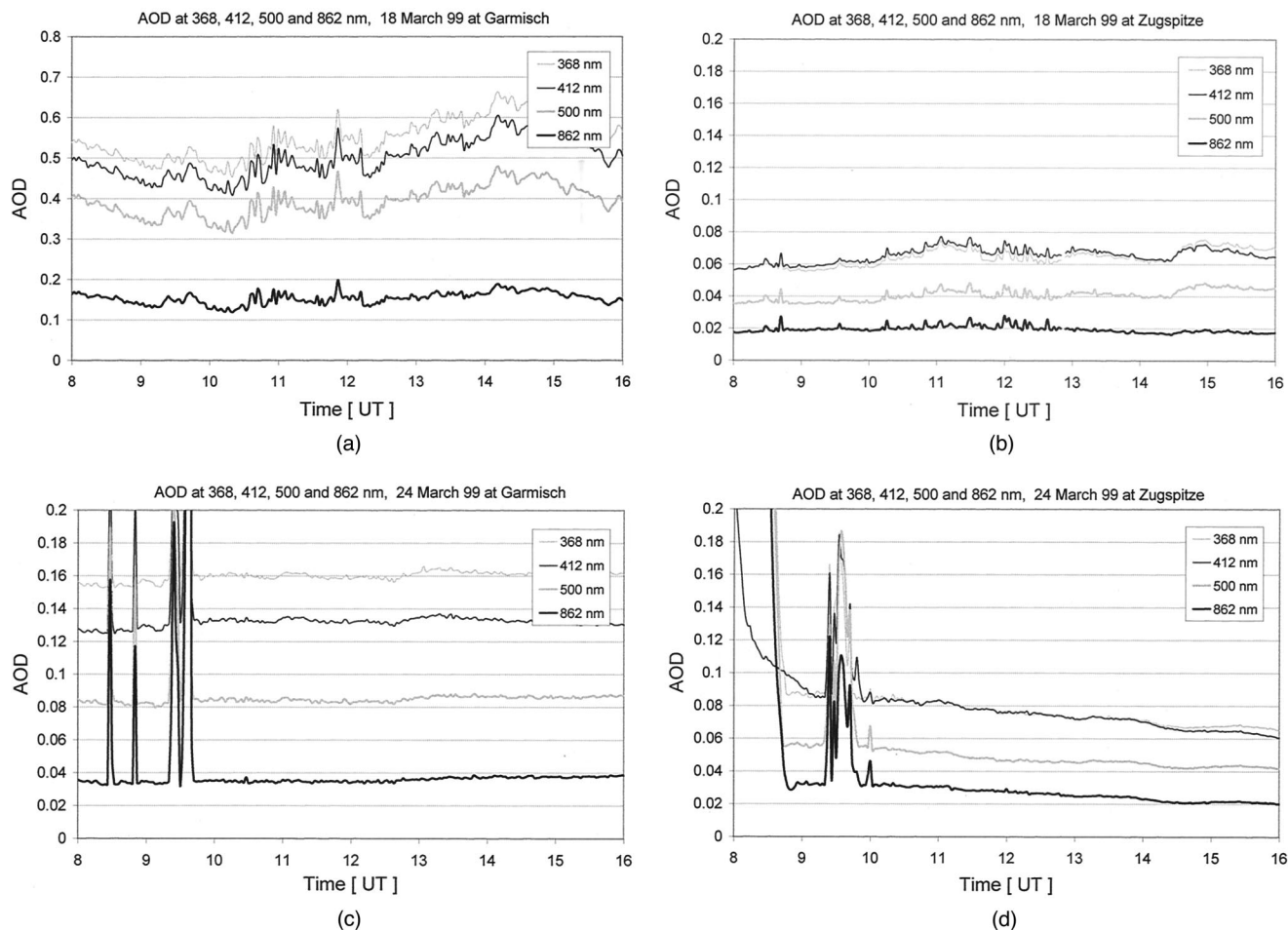


Fig. 2. AOD at four wavelengths, measured by PFRs.

The PFR and the Cimel sunphotometer made simultaneous measurements at Zugspitze on 18 March and in Garmisch on 24 March. The AODs at 400 nm measured by the Cimel agree within 20% with those from the PFR. On 18 March the α values found both

instruments also agreed well. On 24 March in Garmisch the Cimel α was smaller (average 1.21) than the PFR value (1.75). This difference was due partly to the instruments' uncertainties but can also be explained by the facts that an angstrom relationship is

Table 3. Average AODs and Standard Deviations for PFRs^a

Garmisch, 18 March, AOD (400) = 0.515, α = 1.53				
Wavelengths	368	412	500	862
AODs (Average 8–16)	0.551	0.500	0.394	0.154
Standard deviations	0.053	0.048	0.038	0.015
Zugspitze, 18 March, AOD (400) = 0.061, α = 1.49				
Wavelengths	368	412	500	862
AODs (Average 8–16)	0.0643	0.0657	0.0409	0.0195
Standard deviations	0.0053	0.0046	0.0036	0.0020
Garmisch, 24 March, AOD (400) = 0.136, α = 1.75				
Wavelengths	368	412	500	862
AODs (Average 10–16)	0.1608	0.1328	0.0853	0.0363
Standard deviations	0.0017	0.0016	0.0015	0.0015
Zugspitze, 24 March, AOD (400) = 0.069, α = 1.31				
Wavelengths	368	412	500	862
AODs (Average 10–16)	0.0741	0.0731	0.0467	0.0257
Standard deviations	0.0060	0.0069	0.0038	0.0040

^aAOD at 400 nm; angstrom α parameter.

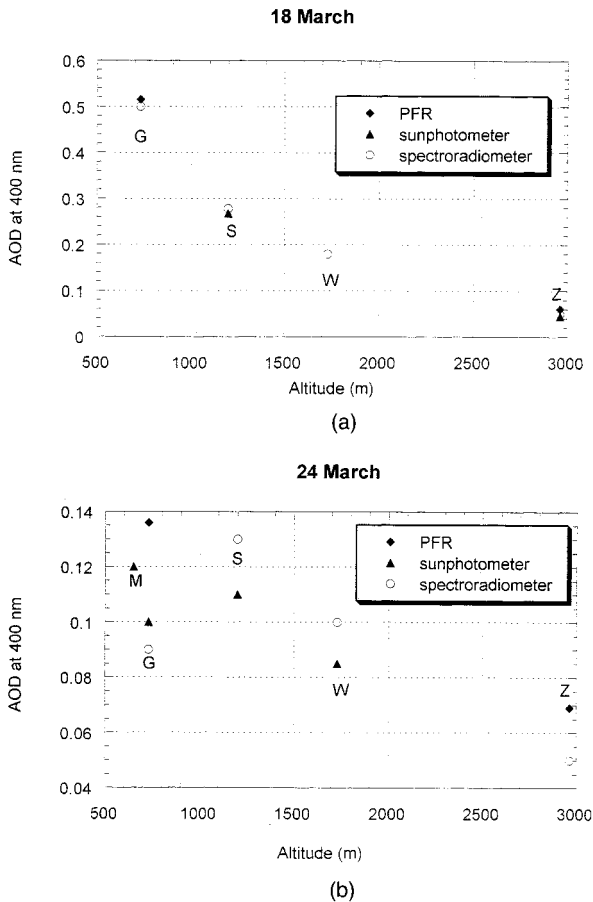


Fig. 3. AOD versus station altitude as measured by various instruments in March 1999: M, for Murnau; G, Garmisch; S, Seefeld; W, Wank; Z, Zugspitze.

only approximate and that the two instruments covered a different wavelength range (see Section 5 below).

3. Microtops Results (Seefeld)

The results for 18 March were averaged over 14 measurements; the AOD at 400 nm was 0.268 ± 0.027 and the angstrom coefficient (fitted for 340–675 nm) was $\alpha = 1.35 \pm 0.08$. For 24 March an average was made of seven measurements and gave for the AOD at 400 nm 0.11 ± 0.03 and $\alpha = 1.38 \pm 0.05$. These values are of the same order as the values given by the PFR and the Cimel instruments at other stations; the differences can be either real atmospheric differences or the differences in wavelength ranges and in the uncertainties of the instruments (Section 5 below). The AOD values are illustrated in Fig. 3.

B. AODs from Spectroradiometers: Comparisons with Filter Radiometer Values

Spectroradiometers provide the spectral distribution of the AOD in the UV between a lower limit in the region 300–330 nm (depending on the instrument) and 400 nm. The spectrum shows oscillations that are due to instrument uncertainties and to the difference in resolution and wavelength alignment be-

Table 4. Summary of Cimel Measurements

Date	Time (UT)	Site	α	β	AOD (400)
10 March	08:10	Garmisch	0.87	0.075	0.166
10 March	08:45	Garmisch	0.48	0.127	0.197
10 March	13:25	Garmisch	1.33	0.060	0.202
13 March	14:15	Murnau	0.63	0.088	0.157
13 March	15:15	Murnau	0.70	0.091	0.172
17 March	08:50	Wank	2.15	0.020	0.143
17 March	09:15	Wank	2.10	0.021	0.144
17 March	14:30	Zugspitze	2.03	0.015	0.096
18 March	07:10	Zugspitze	1.58	0.011	0.047
18 March	08:15	Zugspitze	1.55	0.011	0.046
18 March	11:30	Zugspitze	1.21	0.016	0.048
24 March	07:20	Garmisch	1.33	0.031	0.105
24 March	09:30	Murnau	1.24	0.038	0.118
24 March	12:10	Garmisch	1.10	0.037	0.101
24 March	13:20	Wank	1.10	0.031	0.084
24 March	13:55	Wank	1.07	0.032	0.085
24 March	14:40	Garmisch	1.14	0.037	0.105
24 March	15:30	Garmisch	1.24	0.034	0.105
25 March	06:50	Garmisch	1.45	0.045	0.170
25 March	07:30	Murnau	1.27	0.053	0.170
25 March	10:15	Garmisch	1.33	0.048	0.162
25 March	12:30	Wank	1.19	0.041	0.122

tween the solar extraterrestrial flux and the measurements⁸; the oscillations were smoothed, generally by use of an angstrom fit. As explained above, we shall focus on the value at 400 nm to compare results with the filter radiometer values.

1. Spectroradiometer ATI Operated by the University of Innsbruck at Seefeld

Figure 4 shows an example of AOD spectra observed by the ATI instrument, with a fit to angstrom's law (for some other instruments, the oscillations are much larger than seen here). The slit function of the ATI spectroradiometer (measured with a He–Cd line at 325 nm) was taken into account when we derived the AOD from the direct-Sun measurements and

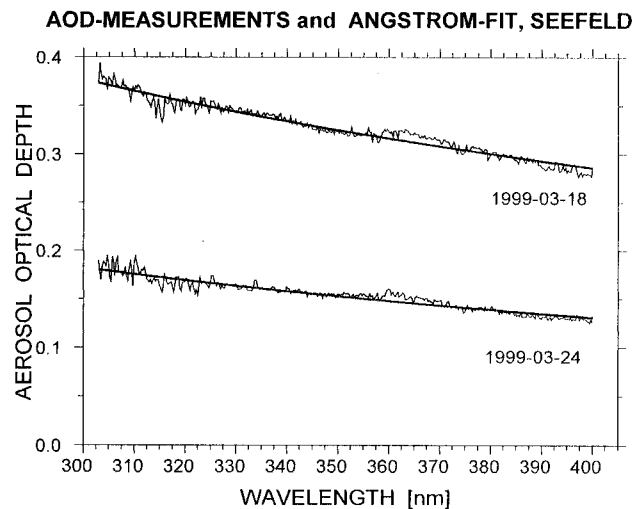


Fig. 4. Examples of ATI spectra with fit to angstrom law at Seefeld on 18 and 24 March 1999.

from a high-resolution extraterrestrial solar spectrum. Furthermore, the wavelength alignment of the spectroradiometer was carefully controlled to be better than ± 0.02 nm. This, combined with an uncertainty of the irradiance calibration estimated to be $\pm 5\%$, resulted in an error of ± 0.03 in the AOD for an air mass of 2. At wavelengths less than 325 nm, we determined amount of ozone by multiple nonlinear regression and deduced its contribution to retrieve the AOD; the high-frequency oscillations were due to the combined influence of various uncertainties.

The average AOD at 400 nm (15 measurements) was 0.278 ± 0.031 on March 18 and (12 measurements) 0.130 ± 0.005 on March 24. These values are shown in Fig. 3 and agree with the Microtops values within the expected uncertainty.

2. Spectroradiometers Operated by the Fraunhofer Institute at Garmisch and Zugspitze

The aerosol optical depth at Garmisch on 18 March as retrieved from spectral measurements showed fairly typical behavior for the site. As the early morning mist is burnt off the optical depth falls, on that day to a value of ~ 0.4 at 400 nm. Then, from 11:00 UT onward, the measured optical depth was seen to increase slowly, reaching a value of 0.6 at 400 nm by late afternoon; data from the PFR show a similar behavior. On 24 March the measurements showed a very low aerosol loading, with optical depths at 400 nm approximately 0.09 for the whole day; again, the PFR shows the same stability, albeit with a larger AOD (0.136 at 400 nm).

On both 18 and 24 March, the aerosol column above the Zugspitze site, which at almost 3000 m lies well above the boundary layer, was negligible compared with the column measured in the valley at Garmisch. Values of the optical depth were typically less than 0.05 for measurements made on each day, also in agreement with the PFR values (differences of 0.01–0.02). The AOD values are shown in Fig. 3.

3. Spectroradiometer Operated by the University of Grenoble at Wank

Direct solar irradiance was obtained as the difference between the global and the diffuse irradiances. The calibration accuracy was evaluated to be $\pm 5\%$ both for the global and for the diffuse irradiance, which corresponded to the agreement in global irradiance among the various spectroradiometers (Subsection 2.C). The data were corrected for wavelength shift and cosine error. The extraterrestrial solar flux taken from the Solar Ultraviolet Spectral Irradiance Monitor⁹ (SUSIM) on the shuttle mission Atmospheric Laboratory for Applications and Science 3 (ATLAS 3) had an uncertainty of $\pm 3\%$. The uncertainty in irradiance measurements was estimated to be $\pm 5\%$, assuming that the air mass and the Rayleigh component were known exactly, the uncertainty in the AOD was 0.04 for an air mass equal to 2; which is larger than for the ATI instrument, because direct irradiance is obtained as the difference between global and diffuse irradiances, leading to addition of

errors. The shadow disk obscured part of the sky radiance and therefore decreased the measured diffuse irradiance and increased the direct irradiance; for clear conditions as at the Wank station, an error in the AOD at 330 nm of approximately -0.01 and at 400 nm of -0.005 , i.e., much smaller than the expected accuracy of 0.04, could occur.

On 18 March the average AOD at 400 nm was 0.18, with a standard deviation of 0.07, somewhat larger than the expected uncertainty of 0.04 evaluated from measurement uncertainties. We in fact observed a variation in the AODs from ~ 0.11 in the morning to 0.30 in the late afternoon; this variation explains the standard deviation to a large extent.

On 24 March and similarly on the morning of 25 March, the AOD at 400 nm was stable, with average values of 0.10 and 0.13, respectively. The corresponding standard deviations were 0.004 and 0.015, much smaller than the expected uncertainty, which confirms the quality of the measurements and the stability of the atmosphere. The spectroradiometer AODs agreed within the expected uncertainties with the values of the Cimel instrument: respectively 0.10 and 0.085 on 24 March and 0.13 and 0.122 on 25 March. The AOD values at 400 nm are shown in Fig. 3.

C. Attempts to Retrieve the Angstrom Parameter from Spectroradiometer AODs

Retrieval of the angstrom parameter was difficult because of the small spectral interval considered (at most 300–400 nm) and because any uncertainty in the spectral AOD is strongly amplified in the α parameter. The analysis performed in detail by the University of Grenoble for the Wank measurements, is presented first.

1. FRG Instrument at Wank

Values of α show large and erratic variations. On 24 March, when the AOD was stable, α had an average value of 0.25, with a standard deviation of 0.30.

We made a test by replacing the ATLAS 3 extraterrestrial spectrum from the Solar Spectrum (SOLSPEC) instrument on board the space shuttle ATLAS 3 but with smaller resolution and a slightly different slope in the UV. The AODs retrieved with the SOLSPEC displayed larger oscillations because of the low resolution; when smoothing was performed based on the angstrom relationship, however, similar AODs were found but with different values for α ; Table 5 lists the results for three days near solar noon. We could obtain similar results by changing the slope of the ATLAS spectrum, or the instrument calibration, by a few percent.

A further cause of error with the FRG instrument is due to the shadow disk, which masks part of the sky radiance that is interpreted as coming from the Sun. A rough evaluation has shown that for a solar zenith of angle (SZA) of $\sim 46^\circ$ (noon value during the Wank campaign) the AOD at 400 nm should be corrected by $+0.7\%$ and the AOD at 330 nm by $+1.5\%$. This is a negligible change for AODs, but it leads to a

Table 5. Comparison of AOD and α Obtained at Wank with ATLAS 3 and SOLSPEC Extraterrestrial Flux (ET)^a

ET Flux	Date					
	18 March		24 March		25 March	
ATLAS	0.140	0.191	0.016	0.100	0.439	0.147
SOLSPEC	0.678	0.195	1.643	0.094	1.477	0.144

^aFor each day. First column, α ; second column, AOD (400).

larger change of α at noon on 18 March from 0.14 to 0.26.

2. ATI Instrument (Seefeld)

Figure 4 shows that a good fit to the spectral distribution is obtained with the angstrom relation. Consistent and realistic values of α can apparently be retrieved from the University of Innsbruck's ATI spectroradiometer, unlike from the instrument of the University of Grenoble (FRG spectroradiometer); the uncertainty in α , evaluated from the measurement uncertainties, is ± 0.3 . The measurement of direct-Sun irradiance with a separate small telescope, instead of the derivation from global and diffuse measurements, which leads to a larger uncertainty in the AOD, could explain the more successful retrieval of α from the ATI than from the FRG instrument. The following average values were found: $\alpha = 1.05 \pm 0.22$ on 18 March and $\alpha = 1.16 \pm 0.16$ on 24 March; they agree, within the expected uncertainty, with the Microtops results at the same station, i.e., 1.35 and 1.38, respectively.

3. DEG and DEZ Instruments

In general, it seems difficult to retrieve a reliable value for the α parameter from the spectral measurements made at Garmisch and Zugspitze with the Fraunhofer Institute instruments (DEG and DEZ, respectively); a detailed analysis, as in the case of the FRG instrument, has not been performed but should most likely lead to the same conclusions.

4. Summary of Results

Figure 3 gives a picture, for the two clear days, of the AOD variation with the site altitude, and it includes the results of all instruments. When AODs were measured at the same site by different instruments, their values at 400 nm agreed within the expected uncertainty.

On 18 March the AODs decreased with altitude [Fig. 3(a)], from ~ 0.5 at the low altitude level to ~ 0.05 at Zugspitze (for 400 nm); this result is expected, as aerosols are generally located in the lower layers of the atmosphere. On 24 March [Fig. 3(b)] the values were much lower (~ 0.11) at low altitude, and therefore the decrease with altitude was much less. On both days the AOD remained of the same order at Zugspitze, with low values, which made the AOD rather difficult to measure accurately. Values of α are more uncertain than the AODs, especially when the AODs are small, as at Zugspitze, or when

they are measured over a narrow spectral range, as by the spectroradiometers. Moreover, the angstrom relation is an approximation, and generally the value of α depends strongly on the spectral interval that is examined.^{10,11} However, the four filter radiometers (Cimel, Microtops, and two PFRs) gave similar values of α of 1.0–1.5; these values correspond to those of continental aerosol, as we discuss in Section 5 below. Among the spectroradiometers, only the ATI instrument permits the retrieval of α .

5. Aerosol Models

A spectral variation of the AOD, measured either by the sunphotometers or by the spectroradiometers, could in principle give some information on the type of aerosol. Assuming spherical particles of radius r , the AOD at wavelength λ can be expressed from Mie theory as

$$\tau(\lambda) = N \int_{r_1}^{r_2} Q_e(m_r, m_i, x) \pi r^2 n(r) dr, \quad (2)$$

where Q_e is a Mie extinction efficiency factor that depends on the real, m_r , and the imaginary, m_i , parts of the refractive index of the particle material and on Mie parameter $x = 2\pi r/\lambda$; $n(r)$ is the normalized size distribution, assumed constant with altitude; and N is the total number of scattering particles in the vertical column. The contributions of particles with radii smaller than r_1 or larger than r_2 are negligible. One can in principle invert Eq. (2) to retrieve the size distribution from the spectral variation of AOD, and much effort has been devoted to doing so. Unfortunately, the inversion problem is ill conditioned, and only limited information, i.e., in the best cases the first moments of the distribution, can be retrieved. Moreover, the spectrum to be inverted must be as extensive as possible, and there is no hope of retrieving the size distribution from the limited UV range observed by the spectroradiometers.

Aerosol models are generally represented by external mixtures of several components, each characterized by its refractive index and a log-normal size distribution (LND),

$$n(r) = (2\pi)^{-1/2} r^{-1} (\ln \sigma)^{-1} \exp[-\ln^2(r/r_m)/2\ln^2 \sigma], \quad (3)$$

where r_m is the mode radius and the variance σ characterizes the width of the size distribution. An important radiative property is the effective radius r_{eff} , defined as an average radius weighted by $r^2 n(r)$. A clean continental aerosol is generally assumed to be a mixture of small water particles that contain various water-soluble compounds (designated WS), such as sulfates and nitrates, and of large dustlike (designated DL) particles, in variable proportions. The materials have similar refractive indices, $m_r = 1.53$ and $m_i \sim 8.10^{-3}$, which increase slightly with wavelength for WS compounds. Table 6 lists the characteristics of two WS and two DL models, proposed respectively

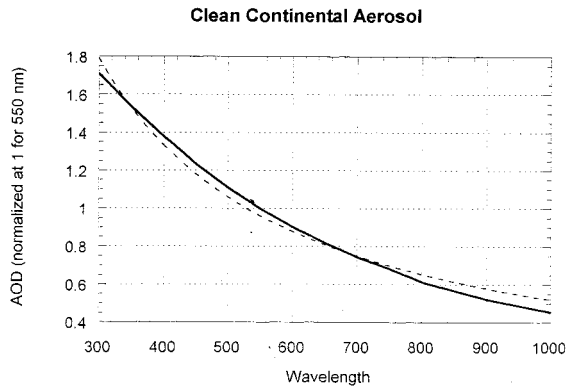


Fig. 5. AOD for a clean continental aerosol model.¹³ Dotted curve, fit to angstrom law: $\alpha = 1.03$.

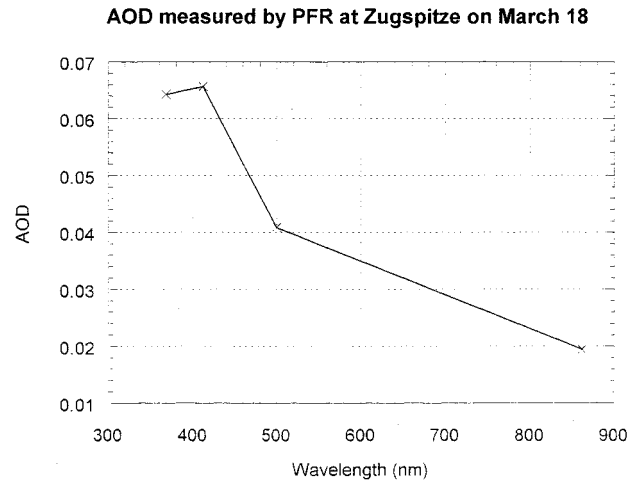
Table 6. Aerosol LND Models

Type	r_m (μm)	σ	r_{eff} (μm)	α	ω
WS1	0.0285	2.239	0.1446	1.11	0.949
WS2	0.005	2.99	0.1003	1.15	0.943
WS3	0.005	2.50	0.0408	1.89	0.936
DL1	0.471	2.512	3.928	-0.09	0.690
DL2	0.5	2.99	10.033	-0.08	0.626
Soot	0.0118	2.00	0.0392	1.33	0.268

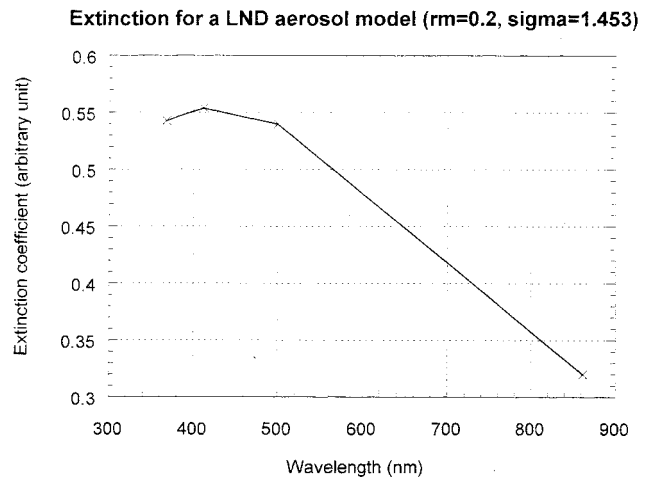
by the International Association for Meteorology and Atmospheric Physics¹² (WS2 and DL2) and d'Almeida *et al.*¹³ (WS1, DL1). We have added a third WS model (WS3), with a smaller r_{eff} . In a continental situation there may be a soot component that is due to pollution; a soot model is also listed in Table 6. Single-scattering albedo ω is given at 400 nm; it varies only slightly with wavelength.

Above, we used angstrom parameter α to give a simple characterization of the AOD spectral variation; α has large values for small particles, with the limit value of four for molecular sizes, and increases to values close to zero (either positive or negative) for large particles. However, the angstrom law is only approximate, and α depends on the spectral interval used for its definition; in Table 6, α is defined in the range 300–1000 nm. For example, in the case of the WS2 component, α in this range is 1.15; in the UV range it is 0.95. Using the PFR channels, we found a value of 1.19, with the Cimel channels, 1.28. It has been found that a best fit of AOD to wavelength on a double-logarithmic scale can often be obtained with a second-order polynomial for biomass burning, desert dust, and urban aerosols¹⁰ as well as for stratospheric aerosols.^{14,15}

In this paper we have limited ourselves to considering the aerosol models that are likely in the Alpine region and could reasonably explain our values of α . Figure 5 represents the spectral variation of the AOD (normalized to 1 at 550 nm) for a clean continental model¹³ made from a mixture of WS1 and DL1 particles in the ratio $10^4:1$; the corresponding volume mixing ratio is 47.5% for WS1 and 52.5% for DL1.



(a)



(b)

Fig. 6. Spectral variations of (a) the AOD and (b) the extinction coefficient for a LND water-soluble aerosol model.

The best fit to an angstrom relationship, over the range 300–1000 nm, gives $\alpha = 1.03$. We found somewhat different values by changing the mixing ratio slightly or the size distribution of one of the components; α also depends on the chosen wavelength interval, as discussed above. Values of α found by PFRs and the Cimel sunphotometer are not unrealistic for a clean continental aerosol.

Gröbner *et al.*,² using a sensitivity study of the global irradiance to the single scattering albedo, found as a best value $\omega \approx 0.95$, which is also consistent with a clean continental aerosol.

A special problem concerns the PFR measurements at Zugspitze; although the α values remained of the same order (1.3–1.5) as at the lower stations, if we look more carefully at the four channel AOD values it appears that the AOD was slightly smaller at 368 nm than at 412 nm on 18 March [Fig. 6(a)]; on 24 March the two values are almost equal. This result has of course to be considered with an expected uncertainty of ± 0.1 for PFR measurements taken into account. However, the change of slope at the short wave-

lengths seems real and is difficult to explain with the clean continental model above; similar behavior has been observed for stratospheric aerosols with a LND of small width.¹⁶ As an illustration, we have drawn in figure 6(b) the spectral distribution of the extinction coefficient computed by Mie theory with such a distribution ($r_m = 0.2 \mu\text{m}$, $\sigma = 1.453$); if it does not exactly reproduce the Zugspitze curve, it presents a similar decrease in the UV range. It is possible that, at the high altitude of Zugspitze, with a clear troposphere, a large part of the small aerosol amount is due to the stratospheric aerosols. Other aerosol models could probably be found that would reproduce the observed behavior. Of course, given the difficulty of measuring the low AOD values at high altitudes, the discussion above has to be considered only tentative.

6. Conclusions

Aerosol optical depth (AOD) was measured at various sites in the German Alps when the Sun was not obstructed by cloud. Results are presented here for 18 and 24 March 1999, two days that were almost completely free of clouds and with substantially different turbidity conditions. These measurements, associated with UV spectral global irradiance measurements at different sites, can give a good insight into the effects of aerosols on UV radiation.

Measurements were performed on the one hand in the UV spectral range (300–400 nm) with spectroradiometers and on the other hand with precision filter radiometers and commercial filter sunphotometers in a broad wavelength range over the visible region from the near UV to the near IR. When two or more instruments operated at the same site, they generally showed good agreement for the AOD at 400 nm (differences, 0.01–0.02). This is an important result, which confirms that one can use either method to retrieve the AOD necessary for modeling UV irradiance and analyzing its effect.

On 18 March the turbidity was quite high (AOD of 0.5 at 400 nm) at low altitude (Garmisch, 730 m asl) and decreased rapidly with altitude to ~ 0.05 at Zugspitze. On 24 March the air was much clearer, with AOD at 400 nm near 0.11 at the IFU. No significant decrease was observed with altitude, except at high altitude (Zugspitze). Diurnal variations were observed on 18 March at some sites (Garmisch, Wank), with turbidity increasing from morning to evening.

To gain some insight into the types of aerosol, we analyzed the spectral distribution of AOD, based mostly on the empirical angstrom relationship. The α parameter was obtained by a best fit of the measurements to the angstrom law and depended slightly on the spectral range of the instrument. Cimel and PFR instruments operating side by side at Garmisch on 24 March and at Zugspitze on 18 March agree to a value of ~ 1.5 in both cases; Microtops at Seefeld yielded similar values for the two days (~ 1.35). For instruments limited to the narrow UV range it has been difficult to retrieve a reliable value; only the ATI spectroradiometer at Seefeld gave α of

1.0–1.2, in quite reasonable agreement with the nearby Microtops. The α values found (1.1–1.5) point to a clean continental aerosol model, with somewhat more small water-soluble particles than in the model proposed by d'Almeida *et al.*¹³

A particular situation was found at the Zugspitze: Although the α value found as a fit over the four channels was not much different from those at the other stations, if one looks more carefully at the 412- and 368-nm channels, it seems that the AOD decreases slightly or at least remains constant in the near UV. This behavior, which has also been observed for stratospheric aerosols, could be explained by aerosol models with a narrow size distribution and rather large particles. From a practical point of view, this means that extrapolating the AOD according to angstrom law given correctly at ~ 400 nm by filter sunphotometers could lead to quite a large error at the short UV wavelengths for high-altitude stations; however this error is less severe because the AOD is quite low in this case, and the aerosol effect is almost negligible. Finally, whatever the effort devoted to the calibration of the instruments, we cannot be sure that the data are absolutely free from any systematic bias. However, the good consistency of our data makes us confident that such a systematic bias, if it exists, is certainly rather small.

Appendix A

The AOD is, as usual,¹⁷ obtained from measurements of the direct solar irradiance, which can be expressed by

$$F = F_0 \exp(-m\tau), \quad (\text{A1})$$

where F_0 is the extraterrestrial solar irradiance and m is the relative air mass. In the case of our measurements, solar zenith angle θ_0 was always smaller than 70° – 75° , and m reduced to $1/\cos \theta_0$, whatever the atmospheric component profile. The total atmospheric optical depth τ is due to molecular Rayleigh scattering τ_{Mol} , aerosols τ_{Aer} (AOD), and gas absorption τ_{Gas} , i.e.,

$$\tau = \tau_{\text{Mol}} + \tau_{\text{Aer}} + \tau_{\text{Gas}}. \quad (\text{A2})$$

Equations (A1) and (A2) are valid only for monochromatic or nearly monochromatic radiation, i.e., over a wavelength range in which the atmospheric properties do not vary significantly; wavelength λ was omitted for simplicity. If the instrument is calibrated on an absolute energy scale and F_0 is known from space observations (as from the SUSIM instrument on the ATLAS 3), τ can be directly retrieved from Eq. (A1); otherwise a relative calibration is performed by the Langley plot method.¹⁷ Outside the gaseous absorption bands, as the molecular component is easily evaluated, τ_{Aer} is derived from Eq. (A2).

From 330 to 400 nm there is no noticeable gas absorption and one can easily obtain the AOD by subtracting the Rayleigh optical depth from the total optical depth. The AOD retrieval can be slightly extended to shorter wavelength by use of the total

ozone amount provided by an external source, e.g., the Total Ozone Mapping Spectrometer, to compute and subtract the ozone optical depth. Another option can be the extrapolation of the AOD below 330 nm and retrieval of the ozone optical depth and total amount from direct solar irradiance measurements.^{18,19}

This study was supported by the European Commission under contract ENV-CT97-0575.

References

1. M. Tevini, ed., *UV-B Radiation and Ozone Depletion: Effects on Humans, Animals, Plants, Microorganisms and Materials* (Lewis, New York, 1993).
2. J. Gröbner, A. Albold, M. Blumthaler, T. Cabot, A. de la Casinière, J. Lenoble, T. Martin, D. Masserot, M. Müller, R. Philippona, T. Pichler, E. Pougatch, G. Rengarajan, D. Schmucki, G. Seckmeyer, C. Sergent, M. L. Touré, and P. Weihs, "The variability of spectral ultraviolet irradiance in an Alpine environment," *J. Geophys. Res.* **105**, 26,991–27,003 (2000).
3. A. Kylling, A. F. Bais, M. Blumthaler, J. Schreder, and C. S. Zerefos, "The effect of aerosols on solar UV irradiances during the PAUR campaign," *J. Geophys. Res.* **103**, 26,051–26,060 (1998).
4. J. E. Hansen and A. A. Lacis, "Sun and dust versus greenhouse gases: an assessment of their roles in global climate change," *Nature* **346**, 713–719 (1990).
5. Y. Kaufman, D. Tanré, H. R. Gordon, T. Nakajima, J. Lenoble, R. Frouin, H. Grassl, B. M. Herman, M. D. King, and P. M. Teillet, "Passive remote sensing of tropospheric aerosol and atmospheric correction for the aerosol effect," *J. Geophys. Res.* **102**, 16,815–16,830 (1997).
6. B. N. Holben, T. F. Eck, I. Slutsker, D. Tanré, J. P. Buis, A. Setzer, E. Vermote, J. A. Reagan, Y. J. Kaufman, T. Nakajima, F. Lavenu, I. Jankowiak, and A. Smirnov, "AERONET, a federated instrument network and data archive for aerosol characterization," *Remote Sens. Environ.* **66**, 1–16 (1998).
7. G. Bernhard and G. Seckmeyer, "Uncertainty of measurements of spectral solar UV irradiance," *J. Geophys. Res.* **104**, 14,321–14,345 (1999).
8. J. Gröbner and J. B. Kerr, "Ground based determination of the spectral ultraviolet extraterrestrial irradiance: providing a link between space-based and ground-based solar UV measurements," *J. Geophys. Res.* **106**, 7211–7217 (2001).
9. R. P. Cebula, G. O. Thuilier, M. E. Vanhoosier, E. Hilsenrath, M. Herse, G. E. Brueckner, and P. C. Simon, "Observations of the solar irradiance in the 200–350 nm interval during ATLAS-1 mission: a comparison among three sets of measurements—SSBUV, SOLSPEC, and SUSIM," *Geophys. Res. Lett.* **23**, 2289–2292 (1996).
10. T. F. Eck, B. N. Holben, J. S. Reid, O. Dubovik, A. Smirnov, N. T. O'Neill, I. Slutsker, and S. Kinne, "Wavelength dependence of the optical depth of biomass burning, urban and desert aerosols," *J. Geophys. Res.* **104**, 31,333–31,349 (1999).
11. N. T. O'Neil, T. F. Eck, B. N. Holben, A. Smirnov, O. Dubovik, and A. Royer, "Bimodal size distribution influences on the variation of Angström derivatives in spectral and optical depth space," *J. Geophys. Res.* **106**, 9787–9806 (2001).
12. Radiation Commission, International Association for Meteorology and Atmospheric Physics, "A preliminary cloudless atmosphere for radiation computation," WCP-112; WMO/TD-No.24 (World Meteorological Organization, Geneva, Switzerland, 1986).
13. G. d'Almeida, P. Koepke, and E. P. Shettle, *Atmospheric Aerosols. Global Climatology and Radiative Characteristics* (Deepak, Hampton, Va., 1991).
14. C. Brogniez and J. Lenoble, "Size distribution of stratospheric aerosols from SAGE II multiwavelength extinctions," in *Aerosols and Climate*, P. V. Hobbs and M. P. McCormick, eds. (Deepak, Hampton, Va., 1988), pp. 305–311.
15. W. P. Chu, M. P. McCormick, J. Lenoble, C. Brogniez, and P. Pruvost, "SAGE II inversion algorithm," *J. Geophys. Res.* **94**, 8339–8351 (1989).
16. C. Brogniez, J. Lenoble, M. Herman, P. Lecomte, and C. Verwaerde, "Analysis of two balloon experiments in coincidence with SAGE II in case of large stratospheric aerosol amount: post-Pinatubo period," *J. Geophys. Res.* **101**, 1541–1552 (1996).
17. G. E. Shaw, A. Reagan, and B. Herman, "Investigations of atmospheric extinction using direct solar radiation measurements made with a multiple wavelength radiometer," *J. Appl. Meteorol.* **12**, 374–380 (1973).
18. M. Huber, M. Blumthaler, W. Ambach, and J. Staehelin, "Total atmospheric ozone determined from spectral measurements of direct solar UV irradiance," *Geophys. Res. Lett.* **22**, 53–56 (1995).
19. G. Seckmeyer, G. Bernhard, B. Mayer, and R. Erb, "High accuracy spectroradiometry of solar UV radiation," *Metrologia* **32**, 697–700 (1996).